

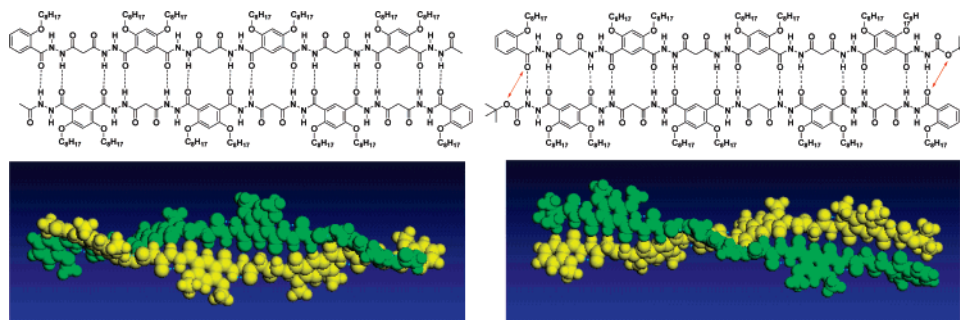
Helical Molecular Duplex Strands: Multiple Hydrogen-Bond-Mediated Assembly of Self-Complementary Oligomeric Hydrazide Derivatives

Yong Yang,^{†,‡} Zhi-Yong Yang,^{†,‡} Yuan-Ping Yi,^{†,‡} Jun-Feng Xiang,[†] Chuan-Feng Chen,^{*,†} Li-Jun Wan,^{*,†} and Zhi-Gang Shuai^{*,†}

Beijing National Laboratory for Molecular Sciences, Institute of Chemistry, Chinese Academy of Sciences, Beijing 100080, China, and Graduate School, Chinese Academy of Sciences, Beijing 100049, China

cchen@iccas.ac.cn

Received March 16, 2007



Careful examination of the X-ray structure of a ditopic hydrazide derivative **7** led to the concept that with malonyl groups as interhydrazide linkers hydrogen-bond-mediated molecular duplex strands might be obtained. Complexation studies between **7**, **8**, and **9** confirmed this hypothesis. Two quadruple hydrogen-bonded heterodimers formed, in which spectator repulsive secondary electrostatic interaction was found to play an important role in determining the stability of the complexes. Extensive studies on **1–4** indicated that the hydrogen-bonding mode could persist in longer oligomeric hydrazide derivatives with chain extension from monomer to tetramer. Molecular duplex strands via two to fourteen interstrand hydrogen bonds were obtained. In addition to affecting the stability of the duplex strands, spectator repulsive secondary electrostatic interaction also played an important role in determining dynamic behavior of the duplex strands as exemplified by variable temperature ¹H NMR experiments. IR studies confirmed stronger hydrogen bonding in the longer oligomers. The assemblies of **1–4** on HOPG were also studied by STM technology. Molecular mechanical calculations further revealed double-helical structures for the longer oligomers. The results provide new opportunities for development of polymeric helical duplexes with well-defined structures.

Introduction

In nature, DNA stores, transfers, and reproduces genetic information. The precise function is based on the self-assembly of two complementary linear strands into a double-stranded complex via hydrophobic effects, hydrogen bonds, and π - π stacking interactions.¹ The assembly of linear proteins into

multistranded complexes through encoded recognition sites is the basis of the behavior of biological fibers such as muscle.² Similar double- and multiple-stranded complexes are ubiquitous in nature,³ which are the foundation for higher structures and functions of biomolecules. Artificial construction of similar structures from unnatural backbones is of fundamental importance for structural mimicking of biomolecules, may shed some light on the understanding of the complicated structures of

* Author to whom correspondence should be addressed. Phone: 86-10-6258-8936. Fax: 86-10-6255-4449.

[†] Beijing National Laboratory for Molecular Sciences.

[‡] Graduate School.

(1) Saenger, W. *The Principles of Nucleic Acid Structure*; Springer-Verlag: Berlin, 1984.

(2) Huxley, H. E. *Science* **1969**, *164*, 1356–1366.

(3) Horton, R. H.; Moran, L. A.; Ochs, R. S.; Rawn, D. J.; Scrimgeour, G. K. *Principles of Biochemistry*; Prentice Hall International, Inc.: London, 1992.

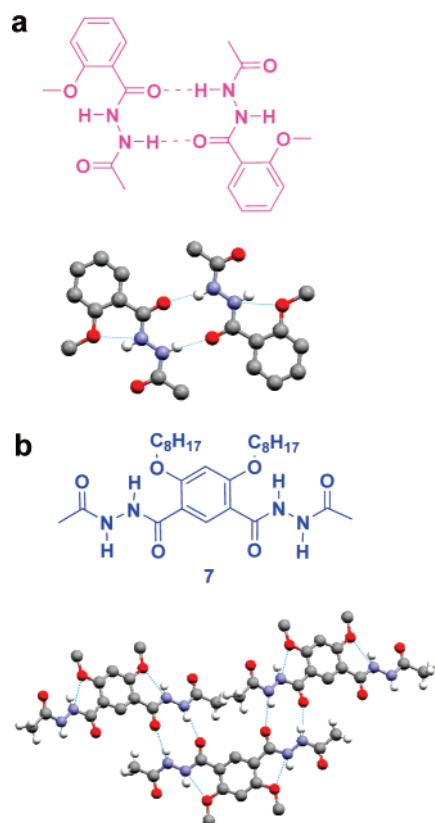


FIGURE 2. Representation of (a) hydrazone-based supramolecular synthon and (b) its application in the construction of supramolecular zipper system from ditopic derivative **7**. The octyl groups are replaced with methyl groups for clarity.

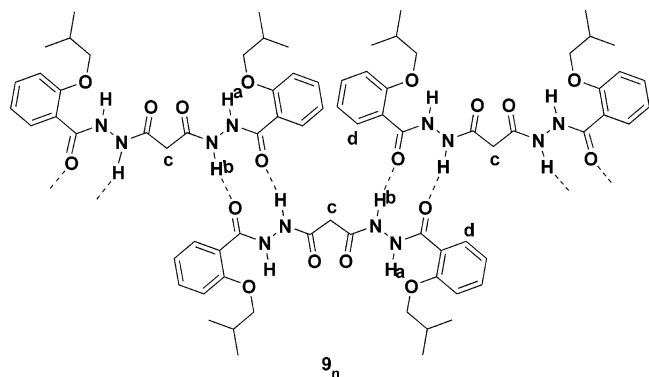


FIGURE 3. Representation of supramolecular zipper structure from **9**.

motifs useful in nanotechnology, nanoscale assembly, and material science and to some extent structural mimicking of DNA.

Results and Discussion

Quadruple Hydrogen-Bonded Heterodimers. Recently, we²⁸ reported a hydrazone-based supramolecular synthon²⁹ and its application in the construction of a supramolecular zipper

(20) (a) Hunter, C. A.; Jones, P. S.; Tiger, P. M. N.; Tomas, S. *Chem. Commun.* **2003**, 1642–1643. (b) Bisson, A. P.; Carver, F. J.; Eggleston, D. S.; Haltiwanger, R. C.; Hunter, C. A.; Livingstone, D. L.; McCabe, J. F.; Rotger, C.; Rowan, A. E. *J. Am. Chem. Soc.* **2000**, *122*, 8856–8868. (c) Bisson, A. P.; Carver, F. J.; Hunter, C. A.; Waltho, J. P. *J. Am. Chem. Soc.* **1994**, *116*, 10292–10293.

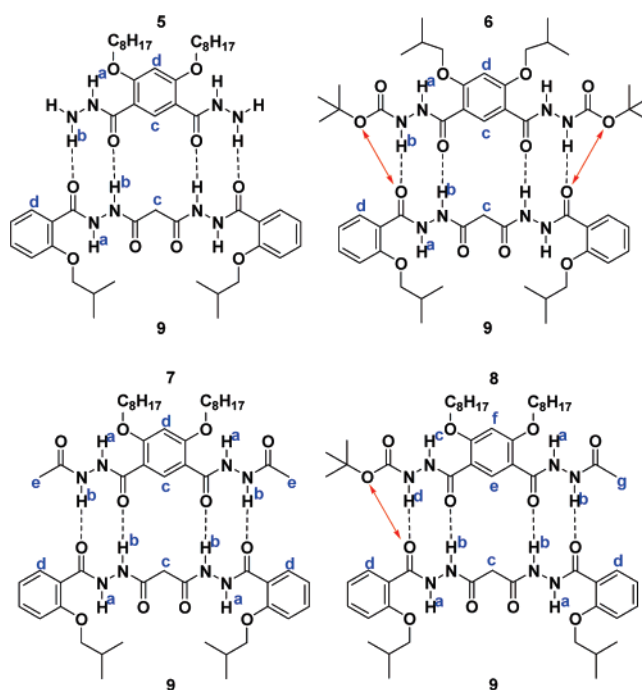


FIGURE 4. Chemical structures of **5**, **6**, **7**, **8**, and **9** and representation of heterodimer structures, with proton-labeling scheme indicated. Spectator repulsive electrostatic interactions are indicated by double headed arrows (red).

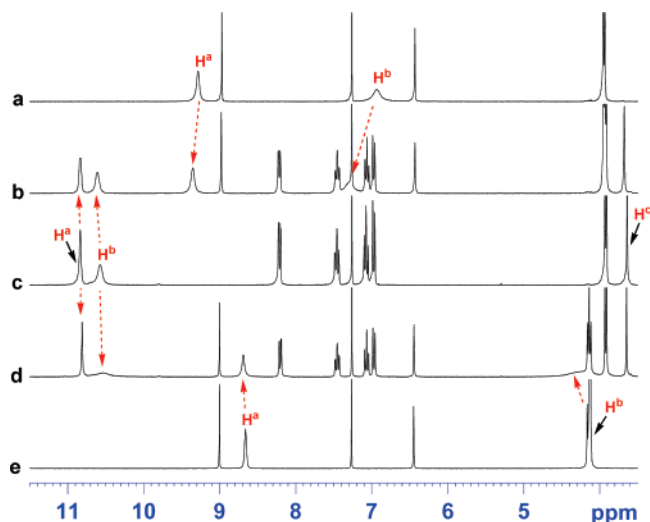


FIGURE 5. Stacked partial ¹H NMR spectra (300 MHz, 25 °C) of (a) **6**, (b) **6** + **9**, (c) **9**, (d) **5** + **9**, and (e) **5**. Each at 20 mM in CDCl₃.

system from ditopic derivative **7**. X-ray analysis indicated that steric hindrance between two adjacent methyl groups rendered

(21) (a) Nowick, J. S. *Acc. Chem. Res.* **1999**, *32*, 287–296. (b) Nowick, J. S.; Chung, D. M. *Angew. Chem., Int. Ed.* **2003**, *42*, 1765–1768. (c) Chung, D. M.; Nowick, J. S. *J. Am. Chem. Soc.* **2004**, *126*, 3062–3063.

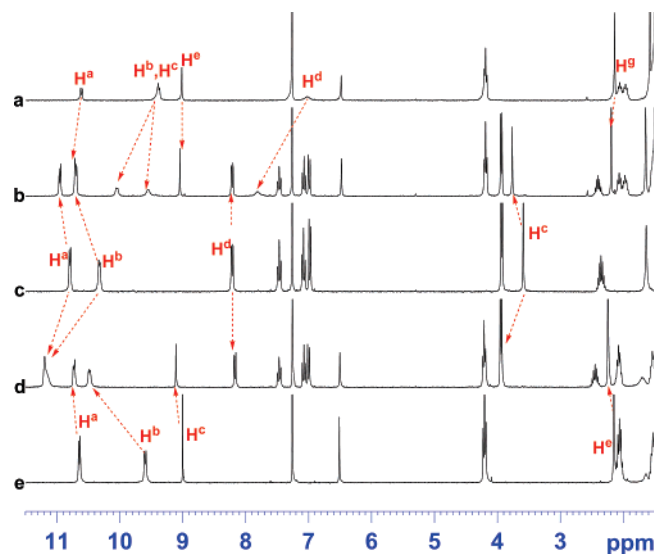
(22) (a) Corbin, P. S.; Zimmerman, S. C. *J. Am. Chem. Soc.* **2000**, *122*, 3779–3780. (b) Corbin, P. S.; Zimmerman, S. C.; Thiessen, P. A.; Hawrylyuk, N. A.; Murray, T. J. *J. Am. Chem. Soc.* **2001**, *123*, 10475–10488. (c) Mayer, M. F.; Nakashima, S.; Zimmerman, S. C. *Org. Lett.* **2005**, *7*, 3005–3008.

(23) Prabhakaran, P.; Puranik, V. G.; Sanjayan, G. J. *J. Org. Chem.* **2005**, *70*, 10067–10072.

(24) Wang, S.-M.; Wu, L.-Z.; Zhang, L.-P.; Tung, C. *Chin. Sci. Bull.* **2006**, *51*, 129–138 and references therein.

TABLE 1. Summary of Complexation Induced Chemical Shifts (CIS, ppm)

	7-H ^a	7-H ^b	7-H ^c	7-H ^e	9-H ^a	9-H ^b	9-H ^c	8-H ^a	8-H ^b	8-H ^c	8-H ^d	8-H ^e	8-H ^g
free	10.64	9.60	9.00	2.15	10.79	10.32	3.59	10.61	9.38	9.38	7.02	9.02	2.14
7·9	10.73	10.48	9.11	2.25	11.20	11.11	3.96						
CIS	0.09	0.88	0.11	0.10	0.41	0.79	0.37						
8·9					10.95	10.70	3.77	10.70	10.04	9.55	7.82	9.05	2.19
CIS					0.16	0.38	0.18	0.09	0.66	0.17	0.80	0.03	0.05

FIGURE 6. Stacked partial ¹H NMR spectra (300 MHz, 25 °C) of (a) 8, (b) 8 + 9, (c) 9, (d) 7 + 9, and (e) 7. Each at 5 mM in CDCl₃.

a dihedral angle of 37.0° between two adjacent aromatic rings (Figure 2). We envisioned that if two methyl carbons converge into one methene carbon, i.e., two hydrazide groups are connected by a malonyl group, multiple hydrogen-bond-mediated supramolecular duplex strands could be expected.

To test this idea, complexation between **5**, **6**, **7**, **8**, and **9** was studied. First, concentration-dependent ¹H NMR spectra of **9** indicated that a supramolecular zipper structure similar to that formed from **7** might form (Figure 3).³⁰ Nonlinear regression analysis^{20b} of the ¹H NMR data of dilution experiments yields an association constant for chain extension of the aggregate of

(25) (a) Wong, C.-H.; Chow, H.-F.; Hui, S.-K.; Sze, K.-H. *Org. Lett.* **2006**, *8*, 1811–1814. (b) Ohkawa, H.; Takayama, A.; Nakajima, S.; Nishide, H. *Org. Lett.* **2006**, *8*, 2225–2228. (c) González, J. J.; Prados, P.; de Mendoza, J. *Angew. Chem., Int. Ed.* **1999**, *38*, 525–528. (d) Rispens, M. T.; Sánchez, L.; Knol, J.; Hummelen, J. C. *Chem. Commun.* **2001**, 161–162. (e) González, J. J.; González, S.; Priego, E. M.; Luo, C.; Guldi, D. M.; de Mendoza, J.; Martín, N. *Chem. Commun.* **2001**, 162–164. (f) Hofmeier, H.; El-ghayoury, A.; Schenning, A. P. H. J.; Schubert, U. S. *Chem. Commun.* **2004**, 318–319. (g) Sánchez, L.; Rispens, M. T.; Hummelen, J. C. *Angew. Chem., Int. Ed.* **2002**, *41*, 838–840. (h) Wang, X.-Z.; Li, X.-Q.; Shao, X.-B.; Zhao, X.; Deng, P.; Jiang, X.-K.; Li, Z.-T.; Chen, Y.-Q. *Chem. Eur. J.* **2003**, *9*, 2904–2913.

(26) (a) Armstrong, G.; Buggy, M. J. *Mater. Sci.* **2005**, *40*, 547–559. (b) Folmer, B. J. B.; Sijbesma, R. P.; Versteegen, R. M.; van der Rijt, J. A. J.; Meijer, E. W. *Adv. Mater.* **2000**, *12*, 874–878. (c) Han, J. T.; Lee, D. H.; Ryu, C. Y.; Cho, K. J. *Am. Chem. Soc.* **2004**, *126*, 4796–4797. (d) Rieth, L. R.; Eaton, R. F.; Coates, G. W. *Angew. Chem., Int. Ed.* **2001**, *40*, 2153–2156. (e) Hoogboom, J.; Swager, T. M. J. *Am. Chem. Soc.* **2006**, *128*, 15058–15059.

(27) Shi, L.; Wang, X.; Sandoval, C. A.; Li, M.; Qi, Q.; Li, Z.; Ding, K. *Angew. Chem., Int. Ed.* **2006**, *45*, 4108–4112.

(28) Yang, Y.; Zhang, Y.-Z.; Tang, Y.-L.; Chen, C.-F. *New J. Chem.* **2006**, *30*, 140–142.

(29) (a) Desiraju, G. R. *Angew. Chem., Int. Ed. Engl.* **1995**, *34*, 2311–2327. (b) Desiraju, G. R. *Chem. Commun.* **1997**, 1475–1482.

(30) See Supporting Information for the details.

$173 \pm 14 \text{ M}^{-1}$. In the 2D NOESY spectrum of **9**, a cross contact between protons of H^c and H^d was observed, which provided a diagnostic evidence for the zipper structure. ¹H NMR studies were then performed on 1:1 mixture of **5** and **9**, each at 20 mM in CDCl₃. The results are summarized in Figure 5. No obvious complexation was observed between **5** and **9**, which might result from low acidity of the unacylated NH₂ protons. To our surprise, only weak association was observed when acylated **6** and **9** (each 20 mM) were mixed in CDCl₃, considering there were quadruple hydrogen bonds. ¹H NMR titration studies failed to give the association constant due to signal broadening and overlapping of NH protons. Strong complexation was observed when **7** and **9**, and **8** and **9**, were mixed (1:1) in CDCl₃, even at a lower concentration (5 mM). The results are summarized in Figure 6. Substantial downfield changes for signal of 9-H^b (0.79 ppm for 7·9 and 0.38 ppm for 8·9), signal of 7-H^b (0.88 ppm), and signals of 8-H^b (0.66 ppm) and 8-H^d (0.80 ppm) were observed. These protons are assumed to participate in intermolecular hydrogen bonding. Signals for protons located along the edges which were assumed to participate in intermolecular interactions all displayed downfield changes (Table 1), especially the signal for 9-H^c (0.37 ppm for 7·9 and 0.18 ppm for 8·9). These downfield changes can be rationalized by assuming these protons lied within the deshielding zone of aromatic ring of another molecule upon complexation. ¹H NMR titration studies³¹ gave association constants of $(1.4 \pm 0.1) \times 10^3 \text{ M}^{-1}$ for 7·9 and $(5.6 \pm 0.6) \times 10^2 \text{ M}^{-1}$ for 8·9, respectively. The differences in association strength could be attributed to additional secondary electrostatic repulsive interactions resulting from spectator^{8a} *tert*-butoxy oxygen atoms and carbonyl oxygen atoms of **9** (depicted by double headed arrows in Figure 4). In complexes 6·9 and 8·9, there exist two and one spectator repulsive interactions, respectively, while in complex 7·9, no spectator repulsive interaction exists.

Variable temperature ¹H NMR studies³⁰ provided additional evidence for the formation of quadruple hydrogen-bonded heterodimer structures. Signals for 9-H^b ($-9.76 \times 10^{-3} \text{ ppm/K}$ in 7·9 and $-1.1 \times 10^{-2} \text{ ppm/K}$ in 8·9), 7-H^b ($-8.88 \times 10^{-3} \text{ ppm/K}$), 8-H^b ($-1.45 \times 10^{-2} \text{ ppm/K}$), and 8-H^d ($-1.81 \times 10^{-2} \text{ ppm/K}$), which involved in intermolecular hydrogen bonding in the complexes, showed large temperature coefficients from 288 to 223 K, while signals for 9-H^a ($-4.79 \times 10^{-3} \text{ ppm/K}$ in 7·9 and $-5.08 \times 10^{-3} \text{ ppm/K}$ in 8·9), 7-H^a ($-1.96 \times 10^{-3} \text{ ppm/K}$), 8-H^a ($-2.88 \times 10^{-3} \text{ ppm/K}$), and 8-H^c ($-3.79 \times 10^{-3} \text{ ppm/K}$), which formed S(6) type³² hydrogen bonds, showed much smaller temperature coefficients within the same temper-

(31) (a) Wilcox, C. S. In *Frontiers in Supramolecular Organic Chemistry and Photochemistry*; Schneider, H.-J., Durr, H., Eds.; VCH: New York, 1991; pp 123–143. (b) Conners, K. A. *Binding Constants: The Measurement of Molecular Complex Stability*; Wiley-Interscience: New York, 1987.

(32) For nomenclature, see: (a) Etter, M. C. *Acc. Chem. Res.* **1990**, *23*, 120–126. (b) Etter, M. C.; Macdonald, J. C.; Bernstein, J. *Acta Crystallogr. Sect. B.* **1990**, *46*, 256–262. (c) Bernstein, J.; Davis, R. E.; Shimoni, L.; Chang, N.-L. *Angew. Chem., Int. Ed. Engl.* **1995**, *34*, 1555–1573.

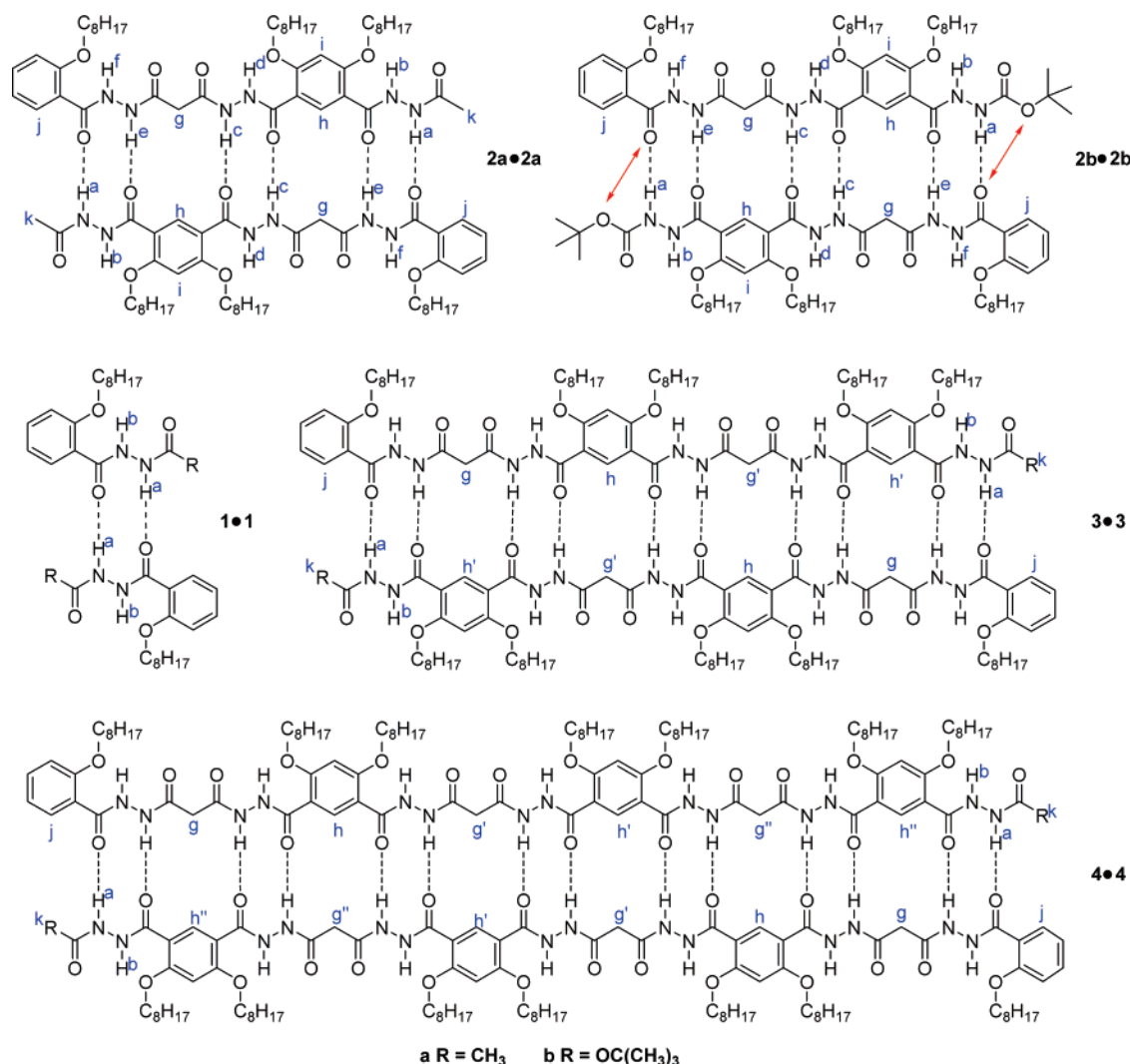


FIGURE 7. Chemical structures of **1–4** and representation of molecular duplex strands, with proton-labeling scheme indicated. Spectator repulsive electrostatic interactions are indicated by double headed arrows (red).

ature range. Small temperature coefficients were also observed for **9-H^c** (-2.63×10^{-3} ppm/K in **7•9** and -3.85×10^{-3} ppm/K in **8•9**).

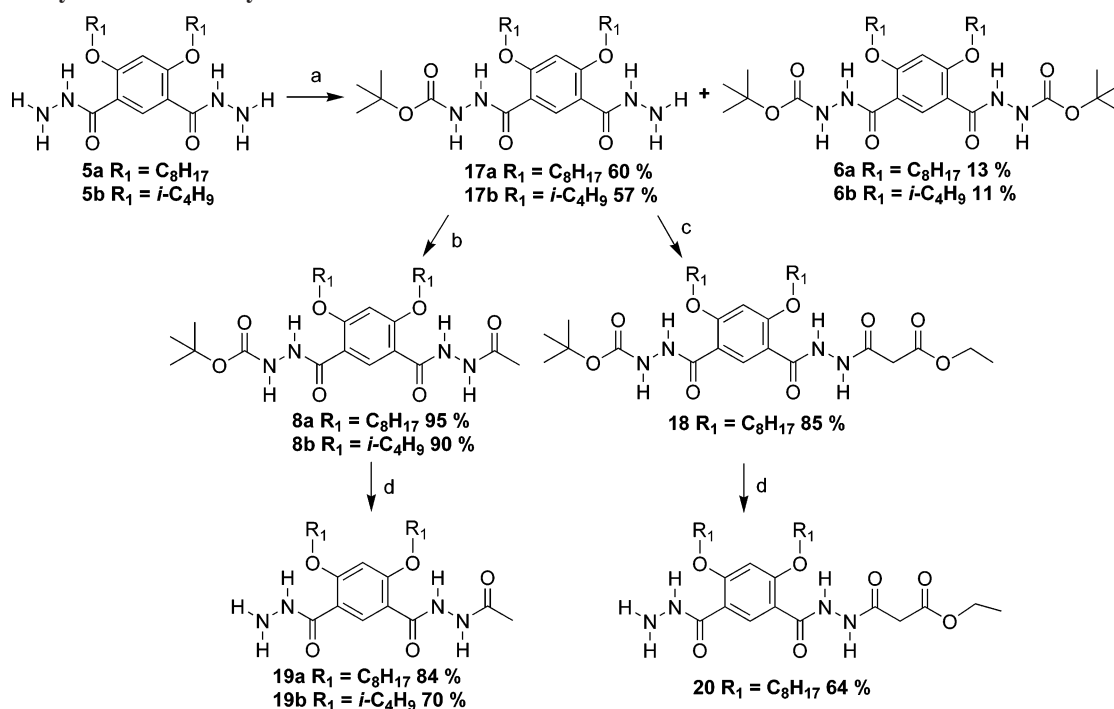
Two-dimensional NMR spectra³⁰ (NOESY, CDCl₃, 300 MHz) provided diagnostic evidence for heterodimer structures. Intermolecular cross-peaks were observed between **7-H^b** and **9-H^b**, **7-H^c** and **9-H^b**, **7-H^c** and **9-H^c**, **7-H^e** and **9-H^d** in a 1:1 mixture of **7** and **9** (each 5 mM), and between **8-H^e** and **9-H^c**, **8-H^e** and **9-H^d** in a 1:1 mixture of **8** and **9** (each 10 mM). The findings are fully consistent with the quadruply hydrogen-bonded heterodimer structures. Another direct evidence for complexation came from ESI-MS (electrospray ionization) studies. When 1:1 mixtures of **7** and **9**, and **8** and **9**, in CH₂Cl₂ and CH₃CN (1:1) were analyzed, signals corresponding to the 1:1 complexes (1041.01 for [**7+9+Na**]⁺, calcd 1041.56; 1098.85 for [**8+9+Na**]⁺, calcd 1099.61) with considerable intensity were found.

Molecular Duplex Strands. Design Strategy and Syntheses.

The results obtained from complexation studies of **7•9** and **8•9** justified the efforts toward preparation of longer molecular duplex strands with malonyl groups as interhydrazide linkers. Compounds **1–4**, which possess one to seven hydrazide motifs and consequently two to fourteen intermolecular hydrogen bonds

in the duplex strands, were therefore designed and synthesized (Figure 7). Incorporation of octyloxy groups should lead to the formation of highly favorable S(6) type hydrogen-bonded rings and therefore rigidify the backbones and preorganize the hydrogen-bonding sites staying in register for the formation of the duplex strands, a strategy extensively used by Gong et al.¹⁷ to rigidify molecular conformation of oligoamide derivatives in the construction of highly stable molecular duplex strands. Another advantage is good solubility of longer oligomers in nonpolar solvent CDCl₃.

Because of their asymmetric structures, an iterative method for the preparation of sequentially homologated oligo(hydrazide) has been devised. The synthetic routes are provided in the Scheme 1 and Scheme 2. For the synthesis of the key intermediates **19** and **20**, a Boc protective/deprotective strategy was adopted for the convenience of product purification. Monoprotected derivative **17** was first synthesized from dihydrazide **5** using equimolar di-*tert*-butyl dicarbonate as acylation reagent and the separation of the product was convenient. Further acylation of **17** was performed efficiently by acetyl chloride in the presence of TEA or by ethyl malonic half ester with 1-ethyl-3-(3-(dimethylamino)-propyl)carbodiimide hydrochloride (EDC•HCl) as coupling reagent. Deprotection of Boc

SCHEME 1. Synthesis of the Key Intermediates **19** and **20**^a

^a Reagents and conditions: (a) Boc₂O/CH₂Cl₂; (b) acetyl chloride/TEA/CH₂Cl₂; (c) EDC·HCl/ethyl malonic half ester/CH₂Cl₂; (d) HCl/AcOEt.

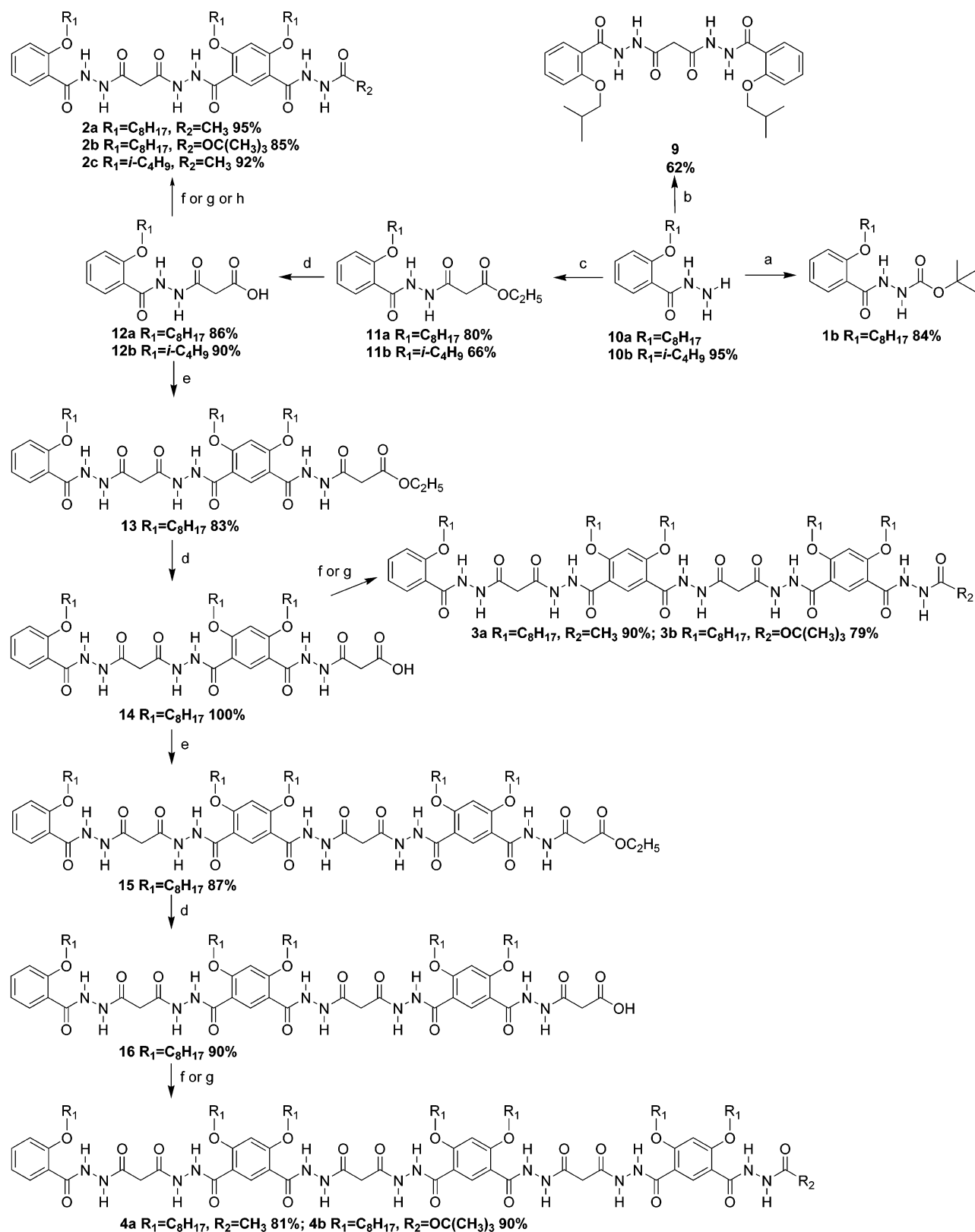
could then be completed using dry HCl in AcOEt to give the compounds **19** and **20**. With them in hand, the oligomers **1–4** could be synthesized efficiently by iteratively applying coupling and hydrolysis steps. EDC·HCl was found to be an efficient reagent for the coupling of carboxylic acid and hydrazide derivatives. Moreover, the hydrolysis step performed well in 1:1 THF and water using NaOH as base. In most cases, purification of the products was convenient, and high yields (ca 90%) were obtained.³⁰

MS Studies. The formation of the duplex strands was first confirmed by mass spectrometry.³⁰ In the ESI-MS of **2a** and **2b**, signals (1671.60 for [**2a**·**2a**+Na]⁺, calcd 1672; 1788.43 for [**2b**·**2b**+Na]⁺, calcd 1788.08) with considerable intensity corresponding to the dimeric structures were observed. Signals (1346.29 for [(**2a**)₃+2Na]²⁺, calcd 1346.81; 1259.36 for [(**2b**)₃+2Na]²⁺, calcd 1259.75) corresponding to the trimeric structures were also observed. For the longer oligomers, whose *m/z* values exceed the detection range of our instrument, MALDI-TOF MS was adopted. Signals corresponding to the dimeric structures were also observed, which might indicate the formation of very stable duplex strands.

¹H NMR Studies. The ¹H NMR spectra of compounds **1–4** are provided in Figure 8 and Figure 9. At 298 K and a concentration of 10 mM in CDCl₃, two NH signals of **1a** appear at 10.95 ppm (H^b) and 9.23 ppm (H^a), respectively. Upon strand extension from monomer **1a** to dimer **2a**, all NH protons exhibit sharp signals in the downfield area (between 11.79 and 10.89 ppm) at the same conditions. These results clearly indicated that all NH protons of **2a** involved in much stronger hydrogen bonding. With the strand extension from dimer **2a** to trimer **3a** to tetramer **4a**, the NH signals all appear between 11 and 12 ppm. No significant downfield shifts were observed, which might mean that a saturation chemical shift change was obtained when the chain length extended to dimer **2a**. The methylene protons of malonyl groups and intercarbonyl aromatic protons

both displayed broad signals (for **3a** and **4a**), which might result from their proximity in space upon complexation as exemplified by 2D NOESY experiments and molecular mechanical calculations (vide infra). Similar results were observed for the *tert*-butoxy-terminated oligomers **1b–4b**. With the strand extension from monomer **1b** to dimer **2b** to trimer **3b**, substantial downfield changes for H^a were observed (from 7.04 to 8.81 ppm to 9.60 ppm). No chemical shift change was observed with strand extension to tetramer **4b**, which might mean a saturation chemical shift change was obtained only when the chain length extended to trimer **3b**. A fit of the chemical shift data³¹ of ¹H NMR dilution experiments in CDCl₃ to a 1:1 binding mode afforded dimerization constants of (1.6 ± 0.1) × 10⁴ M⁻¹, (6.4 ± 1.5) × 10⁴ M⁻¹, and (2.0 ± 0.6) × 10³ M⁻¹ for **1a**·**1a**,²⁸ **2a**·**2a**, and **2b**·**2b**, respectively. No obvious dimerization of **1b** was observed. The differences in association constants strongly suggested that the self-assemblies of **2a**·**2a** and **2b**·**2b** are highly cooperative, and repulsive secondary electrostatic interactions resulting from the spectator^{8a} *tert*-butoxy oxygen atoms and carbonyl oxygen atoms play an important role in determining the stability of the duplex strands. No chemical shift changes were observed when dilution experiments were carried out on the longer oligomers (from 100 mM to 0.5 mM). Considering the cooperative action of 10 and 14 hydrogen bonds and similar chemical shifts of NH protons, the association constants for **3**·**3** and **4**·**4** should be no lower than 10⁵ M⁻¹. ¹H NMR dilution experiments on the longer oligomers in more polar solvents (5% DMSO/CDCl₃ and 5% CH₃CN/CDCl₃) failed to give the association constants due to signal overlapping and small chemical shift changes (<0.1 ppm).

Variable temperature ¹H NMR experiments³⁰ revealed different molecular dynamics for the *tert*-butoxy-terminated oligomers **1b–4b** and methyl-terminated oligomers **1a–4a**. At 228 K and a concentration of 10 mM in CDCl₃, for **2a–4a**, multiple

SCHEME 2. Synthetic Routes for Compounds 1–4 and 9^a

^a Reagents and conditions: (a) Boc_2O/CH_2Cl_2 ; (b) malonic acid/EDC·HCl/ CH_2Cl_2 ; (c) ethyl malonic half ester/EDC·HCl/ CH_2Cl_2 ; (d) i, THF/ H_2O /NaOH; ii, HCl; (e) **20**/EDC·HCl/ CH_2Cl_2 ; (f) **19a**/EDC·HCl, CH_2Cl_2 ; (g) **17a**/EDC·HCl/ CH_2Cl_2 ; (h) **19b**/EDC·HCl/ CH_2Cl_2 .

sets of signals were observed. Especially the NH signals, which appeared in the downfield area between 10.9 and 12.5 ppm at 298 K, exhibited complicated pictures in this field. New minor

signals of NH protons appear in the area between 8 and 9 ppm, which might correspond to NH protons not involved in hydrogen bonding. New signals for malonyl protons also appeared. For

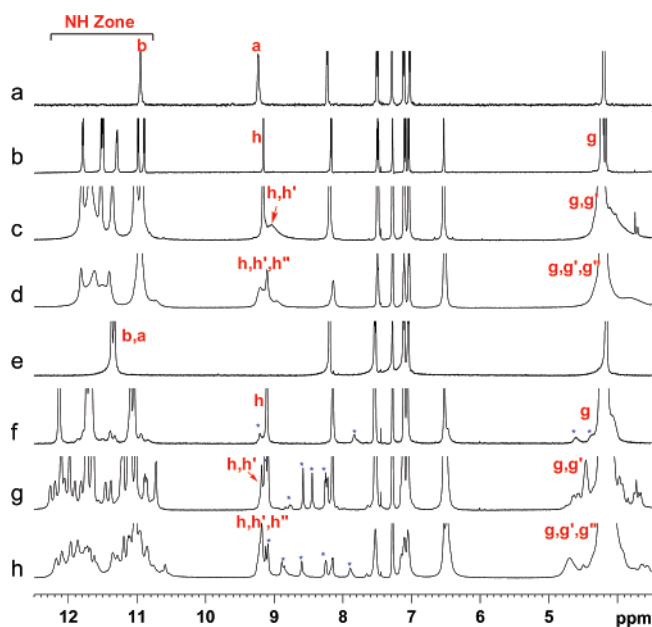


FIGURE 8. Stacked partial spectra of (a) **1a** (5 mM), (b) **2a** (10 mM), (c) **3a** (10 mM), (d) **4a** (10 mM) at 298 K and (e) **1a** (5 mM), (f) **2a** (10 mM), (g) **3a** (10 mM), (h) **4a** (10 mM) at 228 K in CDCl_3 , 600 MHz.

2b–4b at the same conditions, signals for the NH protons only exhibited downfield shifts and sharpening. No new signals were observed. There might exist a dimeric–polymeric equilibrium for the methyl-terminated oligomers.³⁰

2D NMR Studies. Two-dimensional (2D) NMR (NOESY,

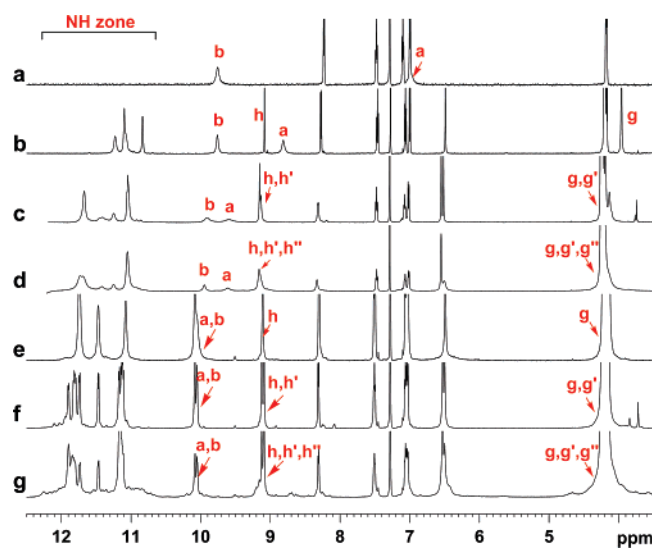


FIGURE 9. Stacked partial spectra of (a) **1b**, (b) **2b**, (c) **3b**, (d) **4b** at 298 K and (e) **2b**, (f) **3b**, (g) **4b** at 228 K, each at 10 mM in CDCl_3 , 600 MHz.

CDCl_3 , 600 MHz) studies provided the most diagnostic evidence for formation of the duplex strands in solution. The results of **2a** (Figure 10) and **2b** (Figure 11) are elaborated below. The NH signals have been assigned by NOESY and TOCSY experiments. For **2a**, important contacts were observed between protons H^k and H^j , H^h and H^c , H^h and H^e , H^a and H^e , and H^h and H^g . Because within the same molecule of **2a** distances between the above-mentioned protons are much too long for

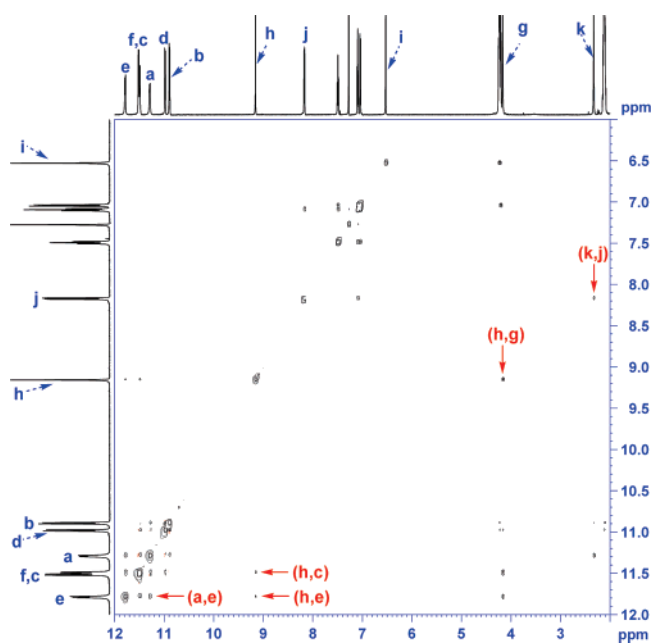


FIGURE 10. NOESY spectrum (10 mM, 600 MHz, 298 K, CDCl_3) of **2a**, with some intermolecular cross contacts highlighted.

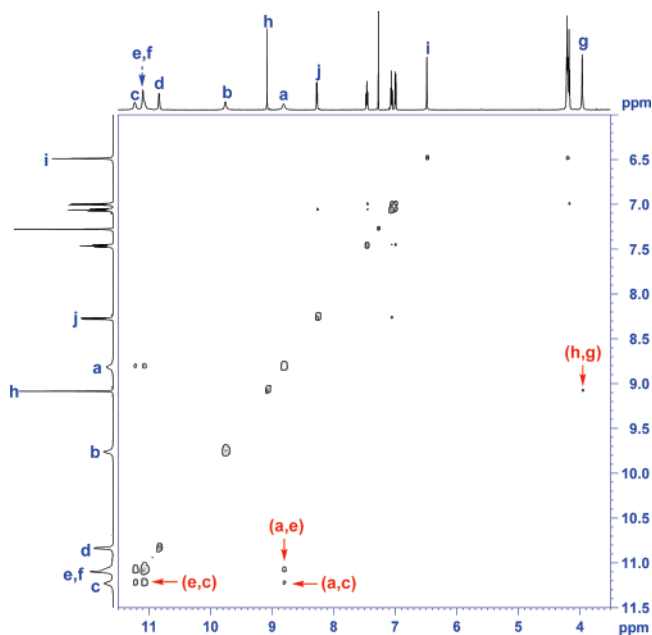


FIGURE 11. NOESY spectrum (10 mM, 600 MHz, 298 K, CDCl_3) of **2b**, with some intermolecular cross contacts highlighted.

any cross-peaks to be observed, the signals must correspond to intermolecular contacts between the two molecules constituting the duplex strands. For **2b**, there are some differences. In addition to cross contacts between H^h and H^g , H^a and H^e , which might result from the centrosymmetric dimeric structure, cross contacts between H^c and H^e , and H^a and H^c , were also observed. There should exist an equilibrium as depicted in Scheme 3. For the longer oligomers, similar results were observed. Cross contacts between H^h ($\text{H}^{h'}$, $\text{H}^{h''}$) and H^g ($\text{H}^{g'}$, $\text{H}^{g''}$), between H^j and H^k for the methyl-terminated oligomers were undoubtedly observed. But we cannot assign NH protons precisely due to signal overlapping. The NOESY and TOCSY spectra were provided in Supporting Information.

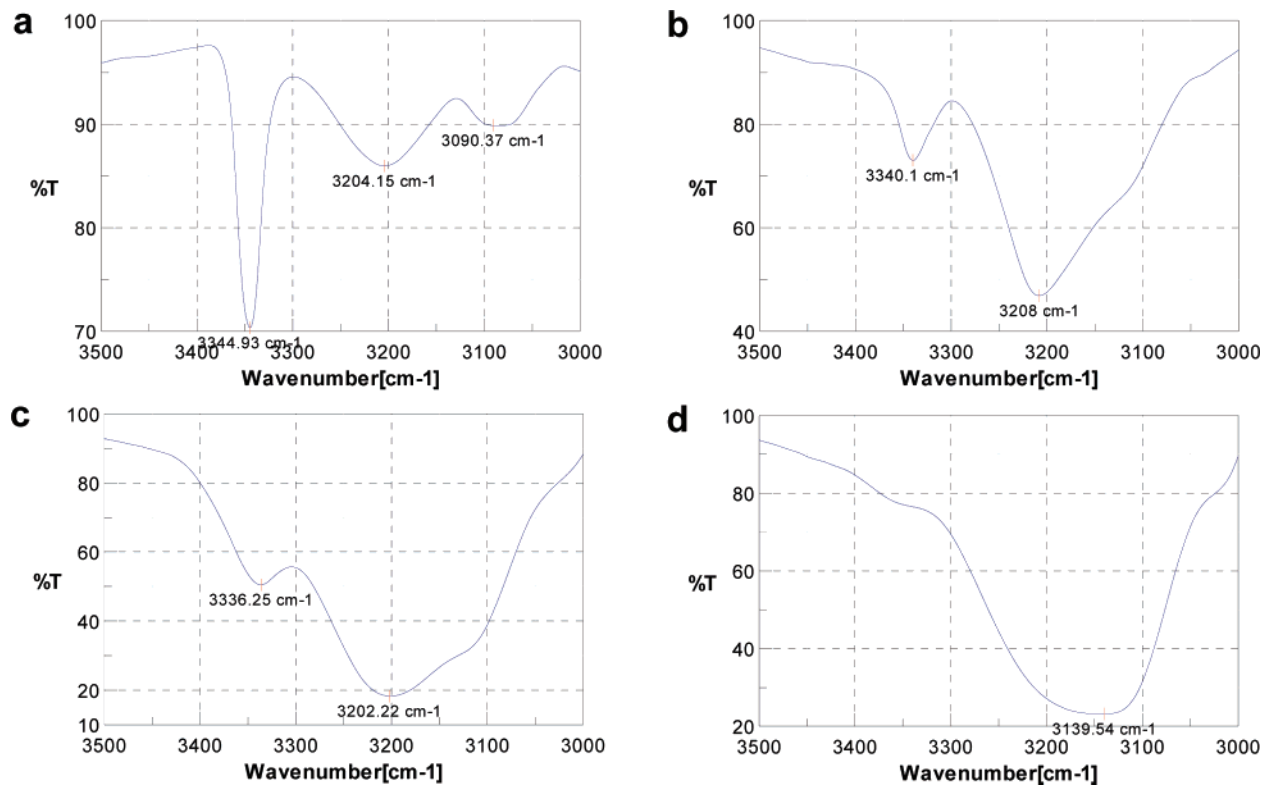
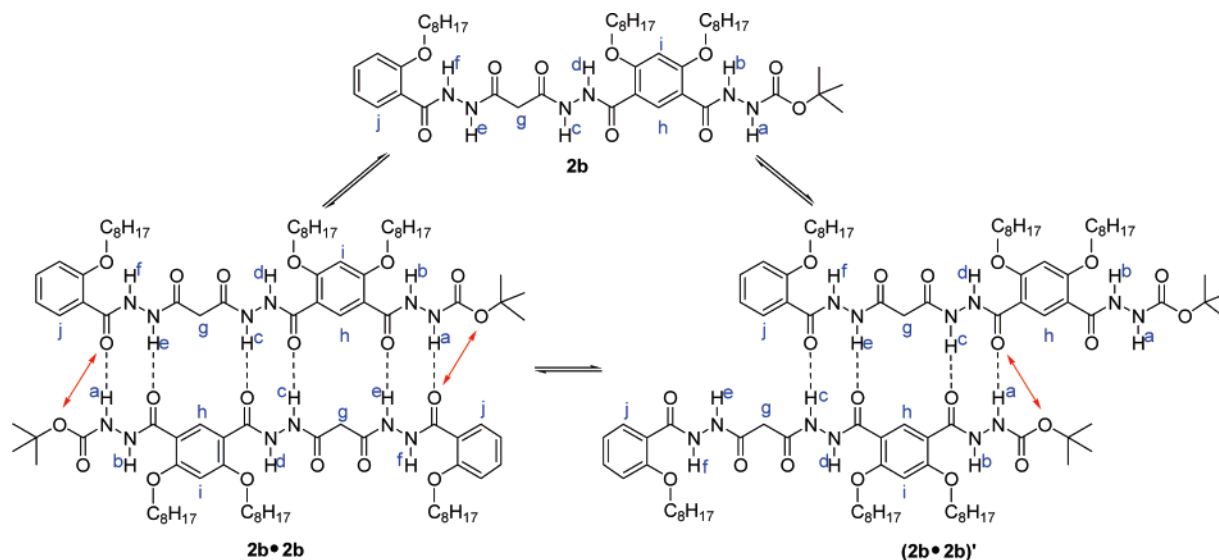


FIGURE 12. Partial IR spectra of (a) 1a, (b) 2a, (c) 3a, and (d) 4a (KBr).

SCHEME 3. Proposed Equilibrium of 2b in CDCl₃



IR Studies. Infrared (IR) spectroscopic data provided additional evidence for the stability of the duplex strands of different chain lengths. Specifically, there were three NH-stretches at 3345, 3204, and 3090 cm⁻¹ in the solid-state (KBr) spectra of 1a. With the strand extension from monomer 1a to dimer 2a to trimer 3a, the intensity of the NH-stretch at ~3340 cm⁻¹ decreased, while the intensity of the hydrogen-bonded NH-stretch increased. When the strand extended to tetramer 4a, no stretch at ~3340 cm⁻¹ was observed (Figure 12). These findings might indicate stronger hydrogen bonding for the longer oligomers. Similar results were observed for the *tert*-butoxy-terminated oligomers. The IR spectra of 1–4 in dry chloroform solution (10 mM) provided similar results as

observed in the solid-state spectra.³⁰ The results clearly showed that the duplex strands formed both in solution and in the solid state.

Calculation. Though attempt to grow a single-crystal suitable for X-ray analysis failed, even with isobutyloxy-substituted derivatives, molecular mechanical calculations provided information on the conformations of the duplex strands. For convenience, the long octyl groups were replaced by methyl groups. The geometries of the compounds were optimized with molecular mechanical method implemented in software programs from Accelrys. Energy-minimization calculations were performed with the Discover program using the COMPASS force field, and the graphical displays were generated with the

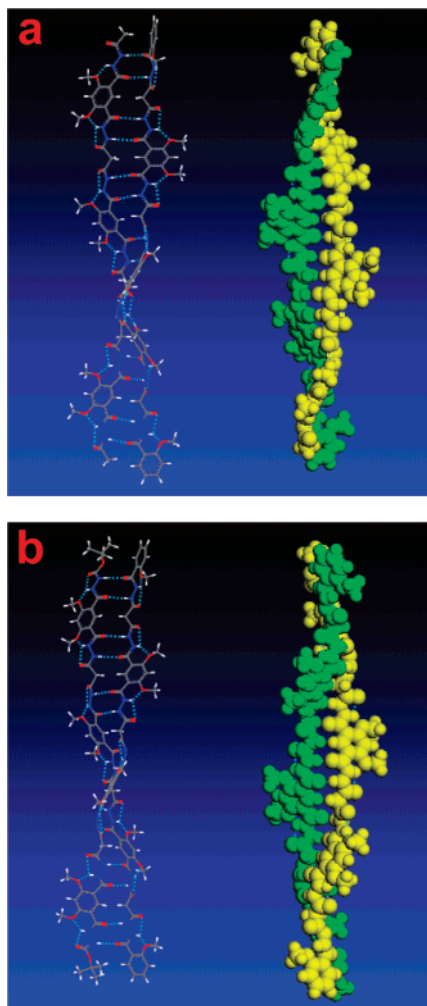


FIGURE 13. Energy-minimized conformations of (a) **4a·4a** and (b) **4b·4b**.

Materials Visualizer.³³ Results for **4a** and **4b** are provided in Figure 13. The S(6) type hydrogen bonds indeed rigidified the backbones. S(5) type hydrogen bonds from NH protons to malonyl oxygen atoms were also presented, which further rigidified the backbones. Docking a single strand with itself revealed that two strands wound up to form a double-helical structure. The methylene protons of malonyl groups and intercarbonyl aromatic protons came into proximity upon dimerization, which was fully consistent with the NOESY experiments. Secondary electrostatic repulsive interactions resulting from spectator *tert*-butoxy oxygen atoms and carbonyl oxygen atoms in **4b·4b** lead to differences in length for the outer hydrogen bonds ($d_{\text{H-O}}$: 1.879 Å for **4a·4a** and 1.933 Å for **4b·4b**).

STM Studies. The self-assemblies of **1–4** on HOPG (high oriented pyrolytic graphite) were also studied by STM (scanning tunneling microscope) technology.³⁴ The results are summarized in Figure 14 and Figure 15. For **1a** and **2a**, the duplex strands were indeed observed. But for **3a** and **4a**, there were no clear

(33) Accelrys, MS Modeling Getting Started, Accelrys Software Inc.: San Diego, 2004.

(34) (a) Giancarlo, L. C.; Flynn, G. W. *Acc. Chem. Res.* **2000**, *33*, 491–501. (b) de Feyter, S.; Gesquière, A.; Abdel-Mottaleb, M. M.; Grim, P. C. M.; de Schryver, F. C. *Acc. Chem. Res.* **2000**, *33*, 520–531.

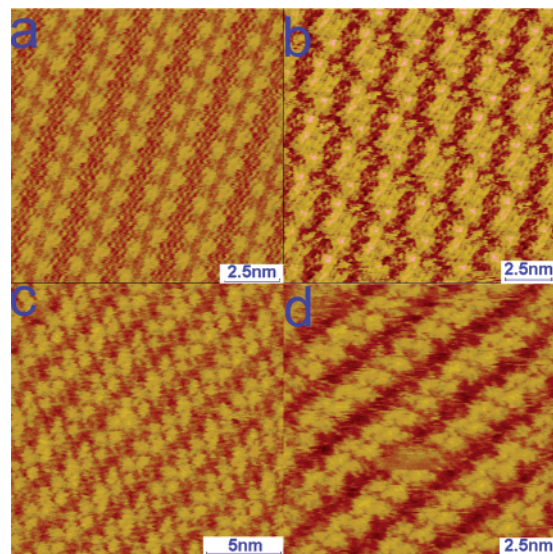


FIGURE 14. STM images of (a) **1a**, (b) **2a**, (c) **3a**, and (d) **4a** on HOPG.

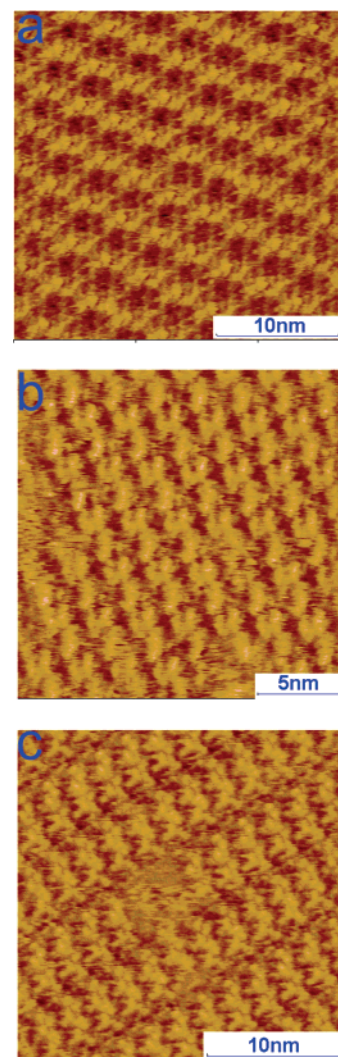


FIGURE 15. STM images of (a) **2b**, (b) **3b**, and (c) **4b** on HOPG.

gaps for the expected duplex strands. Only polymeric duplex strands were observed. These findings probably came from the

different dynamic behaviors in solution and on the surface. For *tert*-butoxy-terminated oligomers **2b** and **3b**, the results are similar to that for **2a**. With chain extension to **4b**, a twisted conformation was observed. These observations are consistent with those of the MM calculations.

Conclusions

Results from model studies of **7·9** and **8·9** led to discovery of a new family of molecular duplex strands from hydrazide-based oligomers with malonyl groups as linkers. Preorganization by intramolecular hydrogen bonding and highly cooperative intermolecular interactions by up to 14 hydrogen bonds resulted in high stability of the duplex stands. Molecular mechanical calculations revealed that two strands wound up to form a double-helical structure, akin to that of DNA. Different dynamical behaviors were also observed for the *tert*-butoxy-terminated oligomers and methyl-terminated oligomers. We believe that the results presented here will provide new opportunities for development of polymeric helical duplexes of well-defined structures and new structural motifs useful in nanoscale assembly, which are underway.

Experimental Section

General Procedure for the Coupling Reaction of Carboxylic Acids and Hydrazide Derivatives (procedure A). To an equimolar mixture of a carboxylic acid and a hydrazide derivative in dry CH₂-Cl₂ (usually 10 mL per mmol) in an ice–water bath was added 1.1 or 1.2 equiv of EDC·HCl. The mixture was stirred at room temperature for 5 h and then concentrated under reduced pressure. The pure product as a white solid was obtained by recrystallization from hot acetonitrile.

General Procedure for Deprotection of Boc Group (procedure B). To a solution or suspension of Boc derivatives in ethyl acetate (usually 10 mL per mmol) was bubbled dry HCl gas for 2 h. After the solvent was evaporated under reduced pressure, the residue dissolved in CH₂Cl₂. The mixture was then neutralized with TEA, washed with water, and dried over anhydrous Na₂SO₄. The crude product was purified by column chromatography (silica gel, usually AcOEt:MeOH = 10:1 as eluent). If necessary, crystallization from hot acetonitrile was used to obtain pure product.

General Procedure for Hydrolysis of Esters (procedure C). To a solution of ester in THF (usually 10 mL per mmol) was added a solution of NaOH (usually 3 equiv) in equivolume of water (relative to THF). Then the mixture was stirred at room temperature, and the reaction was monitored by TLC. The reaction completed in 5 h, and sometimes heating was necessary for the completion of the reaction. The organic solvent was evaporated under reduced pressure, and the residue was acidified with concentrated HCl. Upon acidification, a white solid precipitated from the solution, and the crude product was collected by filtration. The pure product as a white solid was obtained by recrystallization from hot acetonitrile.

Full experimental procedures and characterization data for new compounds are provided in the Supporting Information.

Acknowledgment. We thank the National Natural Science Foundation of China, National Basic Research Program (2007CB808004) and the Chinese Academy of Sciences for financial support.

Supporting Information Available: Experimental procedures and characterization data for new compounds. Detailed information on the evaluation of the duplex strands. This material is available free of charge via the Internet at <http://pubs.acs.org>.

JO070525A